JMATPRO

Journal of Advanced Materials and Processing
12 (46): 33-45, 2024
https://sanad.iau.ir/journal/jmatpro
Doi: 10.71670/jmatpro.2024.1228041

Research Paper

Synthesis, Characterization and Catalytic Application of PVP-Stabilized Pd Nanohybride Using Mesocellular Silica Foam (MCF) as a Sacrificial Template for the Selective Oxidation of Toluene to Benzyl Alcohol

Ali Saffar[*], Hamed Johari, Mahsa Hoseinzadeh Shahiri, Mehdi Nourbakhsh

Department of Chemistry, Na. C., Islamic Azad University, Najafabad, Iran.

ARTICLE INFO

Article history:

Received 03 December 2025
Revised: 24 December 2025
Accepted 07 January 2026
Available online 21 April 2024

Keywords:
Mesocellular foam
Porous organic polymer
Palladium nanoparticles
Selective oxidation

ABSTRACT

In this work, fully organic mesocellular polymer nanohybrids with uniform cellular pores were synthesized via a hard-templating strategy using mesocellular silica foam (MCF) as a sacrificial template. The resulting mesocellular poly(N-vinyl-2-pyrrolidone) (PVP) was subsequently employed as a robust support for finely dispersed Pd nanoparticles (Pd–PVP). The catalyst was comprehensively characterized by XRD, FT-IR, N_2 adsorption–desorption (BET/BJH), TG, SEM, UV–Vis, and TEM analyses. The catalytic performance of Pd–PVP was evaluated in the selective oxidation of toluene to benzyl alcohol under green conditions using aqueous H_2O_2 as oxidant. Under the optimized conditions (H_2O as solvent, K_2CO_3 as base, mild temperature, and low Pd loading), the catalyst showed high conversion and excellent selectivity to benzyl alcohol with negligible over-oxidation. The Pd–PVP catalyst could be readily separated and reused for at least eight consecutive cycles without significant loss of activity or Pd leaching.

Citation: Saffar, A.; Johari, H.; Hoseinzadeh Shahiri, M.; Nourbakhsh, M. (2024). Synthesis, Characterization and Catalytic Application of PVP-Stabilized Pd Nanohybride Using Mesocellular Silica Foam (MCF) as a Sacrificial Template for the Selective Oxidation of Toluene to Benzyl Alcohol, Journal of Advanced Materials and Processing, 12 (46), 33-45. Doi: 10.71670/jmatpro.2024.1228041

---

[*] **Corresponding Author**
E-mail: a.saffar.t@iaun.ac.ir

1-Introduction

The selective oxidation of benzylic C–H bonds is a pivotal transformation in synthetic organic chemistry and industrial oxidation technology, providing access to high-value intermediates such as benzyl alcohol, benzaldehyde, and benzoic acid. From a green chemistry perspective, catalytic oxidation processes that use environmentally benign oxidants (air, O_2, or H_2O_2) and minimize waste are highly desirable [1–3]. Benzyl alcohol is widely used in pharmaceuticals, resins, dyes, and fragrance industries, and its sustainable production via direct oxidation of toluene remains a challenging target due to the inertness of the benzylic C–H bond and the tendency towards over-oxidation.

Homogeneous transition-metal catalysts based on Pd, Ru, Cu, and other metals have shown excellent activity in the oxidation of alcohols and hydrocarbons; however, their industrial deployment is hampered by difficult catalyst separation, metal contamination of products, and limited long-term stability [4–6]. Heterogeneous catalysts circumvent many of these limitations and are easier to recycle, but they often suffer from lower intrinsic activity, mass-transfer limitations, or metal aggregation during use. Recent advances in nanostructured metal catalysts and tailored supports have significantly improved the performance of heterogeneous oxidation catalysts, particularly those based on finely dispersed Pd nanoparticles [7,8].

Poly(N-vinyl-2-pyrrolidone) (PVP) is a widely used stabilizer for noble-metal nanoparticles. PVP strongly coordinates to metal surfaces via carbonyl and nitrogen atoms, controlling particle size, shape, and dispersion [9–11]. PVP-stabilized Pd nanocrystals exhibit enhanced shape stability and resistance to oxidative reshaping, while the polymer shell can modulate the accessibility of active sites and influence reaction selectivity [9,10]. However, in typical colloidal systems PVP remains dissolved in the reaction medium, and the resulting catalysts behave as quasi-homogeneous systems, complicating separation and recycling.

To overcome these limitations, immobilization of Pd–PVP nanoparticles on high-surface-area supports has emerged as an effective strategy. Pd nanoparticles supported on nitrogen-containing ordered mesoporous carbons and carbon nitrides have demonstrated excellent activity in the aerobic oxidation of benzyl alcohol and related substrates, with high selectivities and good recyclability [7,8]. Likewise, various heterogeneous catalyst systems—such as F^--modified hydrotalcites, CeO_2–MnO_x composites, and mixed-oxide supports—have been engineered for the selective oxidation of toluene to benzyl alcohol and benzaldehyde under solvent-free or mild conditions [12–18]. Despite these significant developments, achieving simultaneously high activity, selectivity to benzyl alcohol, and catalyst durability in aqueous media remains non-trivial.

Mesoporous silicas with large, interconnected pore systems have attracted intense interest as robust supports for heterogeneous catalysts. Among them, mesocellular silica foams (MCFs) represent a distinct class of three-dimensional mesostructured silicas composed of large spherical cells connected by uniform windows [19–22]. MCFs combine high surface area, large pore volume, and excellent hydrothermal stability, making them suitable for the immobilization of various catalytic species, including metal nanoparticles, metal oxides, and enzymes. For instance, Pd supported on doped MCF has shown high stability and tunable oxidation states in oxidation reactions, underscoring the potential of MCF-based catalysts [23].

Beyond inorganic silica frameworks, porous organic polymers (POPs) have emerged as a versatile family of materials possessing high surface areas, tunable pore structures, and remarkable chemical and thermal stability. POPs can be designed with specific functional groups and coordination sites, enabling precise control over the microenvironment of embedded metal centers and bridging the gap between homogeneous and heterogeneous catalysis. Recent reviews have highlighted POPs as promising platforms for photocatalysis, CO_2 capture, biomass valorization, and various redox transformations [24–27].

The hard-templating (nanocasting) method provides a powerful route to translate the advantageous architecture of mesoporous inorganic templates into fully organic mesocellular polymers. In this approach, a mesostructured silica (such as SBA-15, KIT-6, or MCF) is used as a hard template; organic monomers infiltrate the pores, polymerize in situ, and the silica is subsequently removed to yield an organic scaffold that replicates the three-dimensional pore architecture of the template [28–30]. Applying nanocasting to MCF thus offers access to mesocellular POPs with large, interconnected pores and controllable composition. Such mesocellular POPs, when loaded with metal nanoparticles, may combine the structural advantages of MCF with the chemical tunability and hydrophobicity of polymers, providing a unique platform for aqueous-phase oxidation catalysis.

Motivated by these considerations, we report here the synthesis of a mesocellular PVP polymer via nanocasting using MCF as a sacrificial template, followed by incorporation of Pd nanoparticles to obtain a Pd–PVP mesocellular nanohybrid. The materials were thoroughly characterized and evaluated as catalysts for the selective oxidation of toluene to benzyl alcohol in aqueous media using

H_2O_2 as oxidant. The influence of the mesocellular polymer framework, reaction conditions, and Pd loading on catalytic activity and selectivity is systematically investigated, and the recyclability and structural stability of the catalyst are demonstrated.

2- Experimental

2-1- Materials

Pluronic P123 (EO_{20}–PO_{70}–EO_{20}), tetraethyl orthosilicate (TEOS), 1,3,5-trimethylbenzene (TMB), N-vinyl-2-pyrrolidone (NVP), divinylbenzene (DVB), benzoyl peroxide (BPO), palladium(II) acetate, hydrazine hydrate (80%), and other reagents were used as received without further purification. Double-distilled water was used throughout all experiments.

2-2- Synthesis of Mesocellular Silica Foam (MCF)

MCF was synthesized following a modified literature procedure [19,20]. Briefly, 2.0 g of Pluronic P123 was dissolved in a mixture of 94.9 mL of 1 M HCl and 75 mL of double-distilled water under vigorous stirring at room temperature to obtain a homogeneous solution. Then, 4.0 g (33.33 mmol) of TMB was added as a swelling agent, and the mixture was stirred at 38 °C for 45 min to form micellar microemulsions. Subsequently, 4.4 g (20.8 mmol) of TEOS was introduced as silica source, and the mixture was stirred at 38 °C for 24 h to promote hydrolysis and condensation. The temperature was then raised to 92 °C, and stirring continued for another 24 h to complete the formation of the mesocellular silica network.

The resulting white gel was filtered under vacuum, washed repeatedly with double-distilled water, and dried overnight at room temperature. The dried solid was calcined in air at 550 °C for 6 h (heating rate 1 °C min^{-1}) to remove the surfactant and obtain the mesocellular silica foam (MCF). The obtained MCF was characterized by XRD, FT-IR, N_2 adsorption–desorption, TG, SEM, and TEM.

2-3- Preparation of PVP/MCF Composite (MCF/PVP)

To prepare the polymer-infiltrated composite, 0.50 g of MCF was charged into a round-bottom flask. NVP (0.50 mL, 4.12 mmol) and DVB (0.061 g, 4.69 mmol) were dissolved in 7 mL of tetrahydrofuran (THF) and added to the flask. The mixture was refluxed at 65–70 °C for 2 h to ensure complete infiltration of monomer into the mesocellular pores. Afterwards, BPO (0.034 g, ~3 mol% relative to total monomer) was added as radical initiator, and polymerization was continued at the same temperature for 10 h.

The resulting cream-colored composite was filtered, washed with THF (2 × 5 mL) to remove non-reacted species, and dried overnight at room temperature to afford the PVP/MCF composite (MCF/PVP), which was characterized by XRD, FT-IR, N_2 adsorption–desorption, TG, SEM, and TEM.

2-4- Synthesis of Mesocellular PVP Polymer

The silica template was removed from MCF/PVP by etching with aqueous HF. The composite (0.50 g) was dispersed in 50 mL of 10% HF solution and stirred at room temperature for 6 h. The resulting polymer was filtered and washed three times with 10% HF to ensure complete dissolution of the silica framework, followed by copious washing with water to remove residual fluoride. The solid was then dried at room temperature to yield the mesocellular PVP polymer. All operations involving HF were conducted under strict safety protocols.

The obtained mesocellular PVP was characterized by XRD, FT-IR, N_2 adsorption–desorption, TG, SEM, and TEM analyses.

2-5- Synthesis of Pd–Mesocellular PVP Nanohybrid (Pd–PVP)

For the preparation of the Pd–PVP nanohybrid, 0.25 g of mesocellular PVP was suspended in 10 mL of chloroform containing palladium(II) acetate (0.0132 g, 0.059 mmol; 0.09 M). The suspension was stirred at 80 °C under nitrogen for 5 h to allow coordination of Pd^{2+} ions to the amide groups of PVP. Subsequently, hydrazine hydrate (0.15 mL, 9.89 mmol, 80%) was added dropwise over 15–20 min as reducing agent and the mixture was stirred at 60 °C for an additional 1 h.

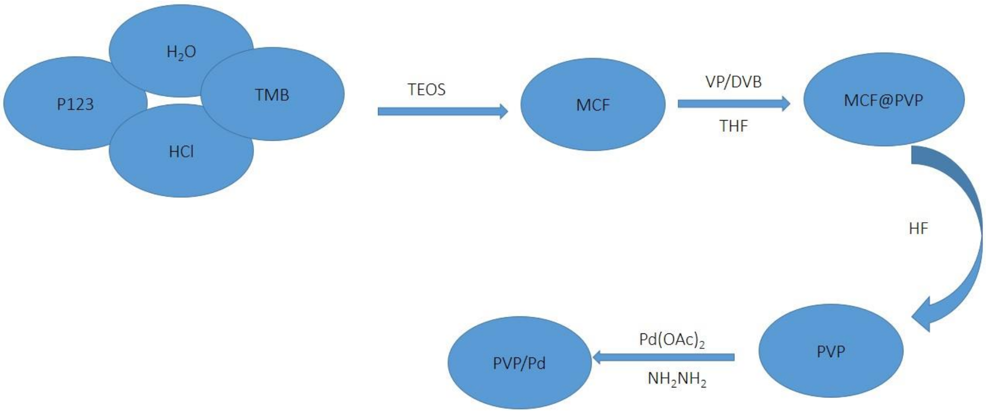

Fig. 1. Synthesis route of Pd-PVP nanocomposite

The resulting black solid was collected by vacuum filtration, washed thoroughly with chloroform and methanol to remove excess hydrazine and by-products, and dried at room temperature. The Pd loading was determined by ICP-AES. The nanohybrid catalyst (Pd–PVP) was characterized by XRD, FT-IR, N_2 adsorption–desorption, TG, UV–Vis, SEM, and TEM.

2-6- Catalytic Oxidation of Toluene to Benzyl Alcohol

The catalytic performance of Pd–PVP was evaluated in the oxidation of toluene to benzyl alcohol using H_2O_2 as oxidant. In a typical experiment, toluene (1 mmol), Pd–PVP (10–30 mg), base (K_2CO_3 or other as specified), oxidant (5 mmol of 30% H_2O_2 or TBHP), and 5 mL of solvent (water, ethanol, acetonitrile, dioxane, or water/ethanol mixtures) were placed in a glass reactor equipped with a magnetic stirrer and reflux condenser. The reaction mixture was heated at the desired temperature (room temperature to 80 °C) under air or nitrogen atmosphere as required.

Reaction progress was monitored by thin-layer chromatography (TLC) and periodic sampling. Aliquots were extracted with dichloromethane, dried over anhydrous Na_2SO_4, and analyzed by GC. After completion, the catalyst was separated by filtration, washed with dichloromethane and water, and dried for reuse.

To examine catalyst recyclability, the recovered Pd–PVP was reused in successive runs under the same optimized conditions. The Pd content before and after recycling was determined by ICP-AES.

3- Results and Discussion

3-1- Synthesis and Structural Features of the Pd–PVP Nanohybrid

The Pd–PVP nanohybrid was obtained through a sequential process: (i) polymerization of NVP and DVB within the mesocellular MCF scaffold to produce PVP/MCF; (ii) HF etching to remove the silica template and yield a mesocellular PVP framework; and (iii) coordination of Pd^{2+} ions to the PVP network followed by hydrazine reduction to generate Pd^0 nanoparticles. This synthetic route effectively combines the architectural advantages of MCF with the stabilizing effect of PVP on Pd nanoparticles.

The resulting Pd–PVP nanohybrid benefits from the presence of amide carbonyl and nitrogen functionalities, which serve as anchoring sites for Pd^{2+} ions and strongly coordinate Pd^0 nanoparticles [9–11]. The mesocellular structure provides interconnected pores that facilitate diffusion of reactants and products, minimize internal mass-transfer limitations, and promote homogeneous dispersion of active sites.

3-2- XRD Analysis

Wide-angle XRD patterns of MCF, PVP/MCF, mesocellular PVP, and Pd–PVP are depicted in Figure 2. In the 2θ range of 10–80°, pure MCF shows only a broad halo characteristic of amorphous silica, consistent with its disordered wall structure, while its small-angle reflections (below 0.5°) lie outside the detection range of the instrument [19,20]. A similar broad background is observed for PVP/MCF and mesocellular PVP, reflecting the amorphous nature of the polymer network.

In contrast, the pattern of Pd–PVP exhibits distinct diffraction peaks at 2θ = 39.9°, 46.5°, 67.9°, and 81.8°, corresponding to the (111), (200), (220), and (311) planes of face-centered cubic (fcc) Pd^0, respectively. The absence of additional peaks associated with crystalline PdO suggests that the reduction of Pd^{2+} to Pd^0 proceeded efficiently and that the metallic nanoparticles are stabilized within the polymer framework. The preservation of an amorphous background indicates that the mesocellular PVP scaffold retains its structural integrity upon metal incorporation.

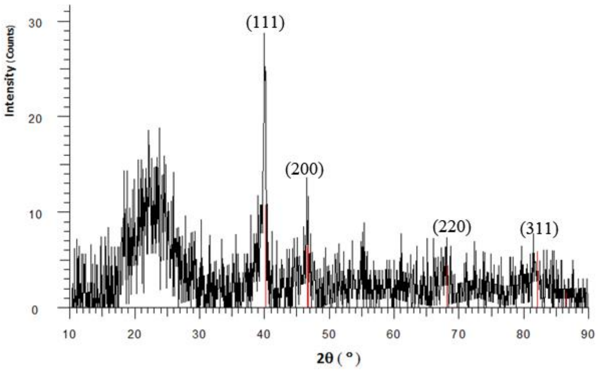

Fig. 2. X-ray Diffraction (XRD) Pattern of Pd-PVP/MCF

3-3- FT-IR Spectroscopy

The FT-IR spectra of MCF, PVP/MCF, mesocellular PVP, and Pd–PVP are shown in Figure 3. For MCF and PVP/MCF, intense bands at 1080, 816, and 458 cm⁻¹ are assigned to asymmetric stretching, symmetric stretching, and bending modes of Si–O–Si, while the band at 950 cm⁻¹ is attributed to surface Si–OH groups, confirming the siliceous framework [19,21].

After in situ polymerization of NVP and DVB inside the MCF pores, a new band emerges at 1663 cm⁻¹, corresponding to C═O stretching of the PVP amide groups, along with a band at 1424 cm⁻¹ related to aromatic ring and CH_2 bending vibrations from DVB, and C–H stretching bands in the 3000–2800 cm⁻¹ range. These features confirm the successful formation of a cross-linked PVP network within the MCF structure.

Upon template removal, the Si–O–Si and Si–OH bands disappear, and the spectrum of mesocellular PVP is dominated by the PVP-related C═O and CH_2/aromatic vibrations, indicating complete dissolution of the silica framework and retention of a stable organic mesocellular polymer. In the Pd–PVP nanohybrid, the C═O stretching band shifts from 1663 to 1639 cm⁻¹ and decreases in intensity, reflecting coordination of Pd nanoparticles to the carbonyl groups and partial weakening of the C═O bond [9–11]. This shift provides strong evidence for the formation of Pd–PVP coordination complexes in the nanohybrid.

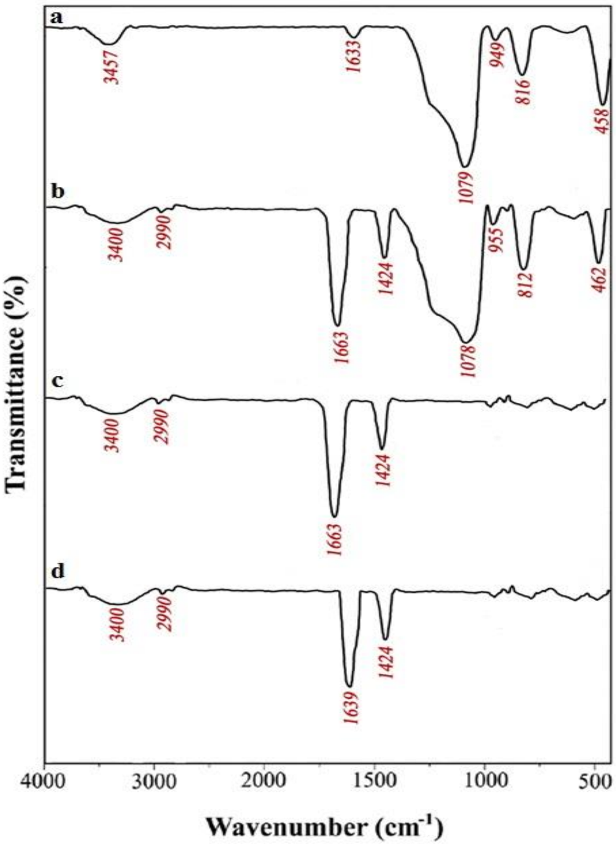

Fig. 3. FT-IR Spectra: (a) MCF, (b) PVP/MCF, (c) Mesocellular PVP, (d) Pd-PVP Nanohybrid

3-4- N_2 Adsorption–Desorption and Textural Properties and Pore Size Distribution

Nitrogen adsorption–desorption isotherms of MCF, PVP/MCF, mesocellular PVP, Pd–PVP and pore-size distribution curves are presented in Figures 4–6. All materials exhibit type IV isotherms with H4-type hysteresis loops, characteristic of mesoporous structures with slit-like or ink-bottle-type pores [21,22].

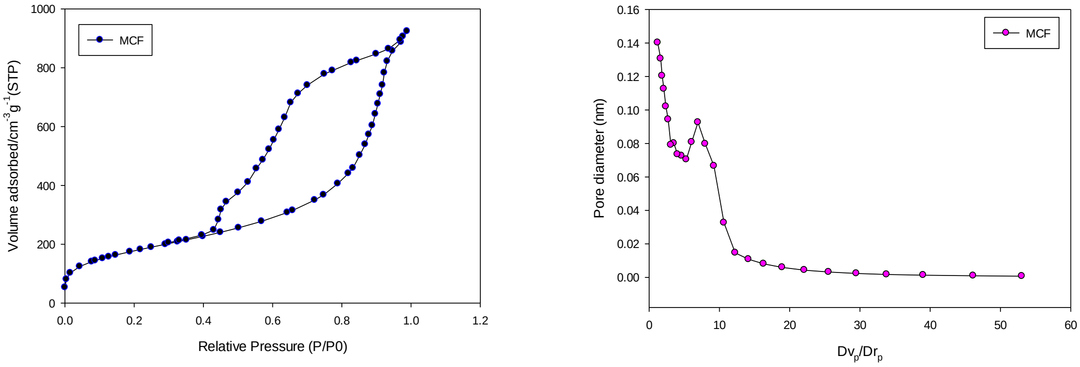

Fig. 4. Nitrogen Adsorption–Desorption Isotherm of MCF and Pore Size Distribution of MCF

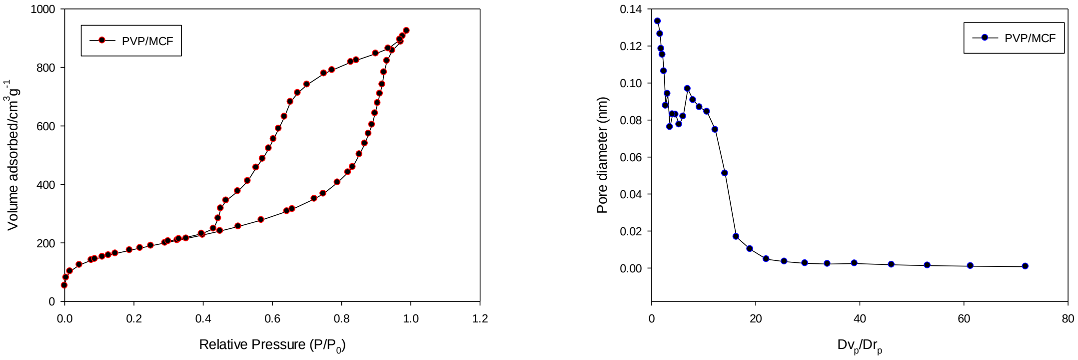

Fig. 5. Nitrogen Adsorption–Desorption Isotherm of PVP/MCF and Pore Size Distribution of PVP/MCF

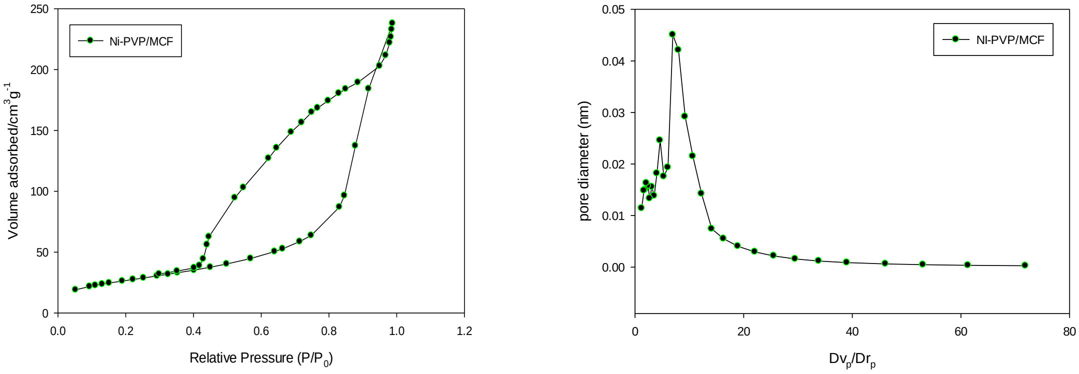

Fig. 6. Nitrogen Adsorption–Desorption Isotherm of Mesocellular Pd-PVP and Pore Size Distribution of Pd-PVP

For MCF, a high BET surface area of 692 $m^2 g^{-1}$, a pore volume of 1.07 $cm^3 g^{-1}$, and an average pore diameter of 6.23 nm are obtained (Table 1), consistent with literature reports for mesocellular foams [19,21]. After polymerization, the PVP/MCF composite shows a slightly reduced surface area (634 $m^2 g^{-1}$) and modified pore parameters, indicating partial filling of mesocellular pores by the polymer chains.

Table 1. Physicochemical Properties of MCF, PVP/MCF, PVP, and Pd-PVP Determined from N_2 Adsorption–Desorption Analysis

Sample	Surface Area (m^2/g)	Pore Volume (cm^3/g)	Pore Diameter (nm)
MCF	692	1.07	6.23
PVP/MCF	634	1.42	9
Pd-PVP	97	0.36	15.7

For the Pd–PVP nanohybrid, the surface area, pore volume, and average pore diameter are 97 $m^2\ g^{-1}$, 0.36 $cm^3\ g^{-1}$, and 15.7 nm, respectively, reflecting partial occupation of pores by Pd nanoparticles and slight reorganization of the polymer framework.

Importantly, the pore-size distribution remains narrow and centered in the mesopore range for all materials, and the Pd–PVP sample preserves a well-defined mesocellular structure, which is crucial for efficient reactant diffusion and catalyst accessibility.

3-5- Thermogravimetric Analysis (TGA)

TG curves of MCF, PVP, and Pd–PVP (Figure 7) provide insights into the thermal stability and composition of the materials. The MCF sample displays a minor weight loss (~7.5%) around 100 °C due to desorption of physically adsorbed water from the surface and pores.

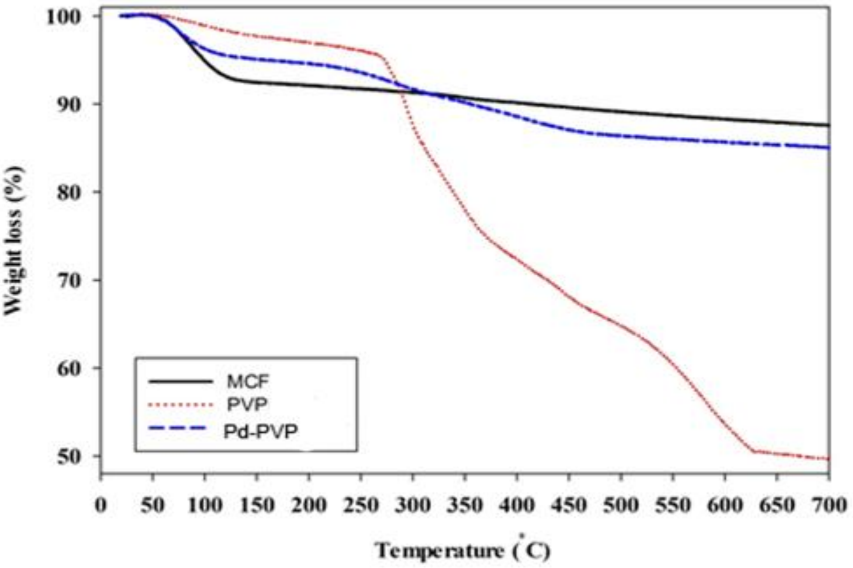

Fig. 7. Thermogravimetric Analysis (TGA) Curves of MCF, PVP, and Pd-PVP

The PVP polymer exhibits two main weight-loss stages: a small loss (~2%) near 100 °C from removal of adsorbed water, followed by a major loss (~48%) between 270 and 630 °C corresponding to thermal degradation of the polymer backbone. In the case of Pd–PVP, the high-temperature weight loss is markedly reduced, indicating that the presence of Pd nanoparticles enhances the thermal stability of the polymer, likely through strong interactions between Pd and the carbonyl/nitrogen functionalities [9–11]. This improved stability is beneficial for catalytic applications at elevated temperatures and confirms the formation of a robust metal–polymer hybrid.

3-6- SEM and TEM Analyses

SEM images of MCF (Figure 8) clearly reveal spherical mesocellular domains and a foam-like morphology, in agreement with typical MCF structures [19,21]. At higher magnification (Figure 8), MCF, PVP/MCF, mesocellular PVP, and Pd–PVP all exhibit similar mesocellular morphologies, indicating that polymerization and template removal do not collapse the overall architecture. The presence of PVP and Pd does not significantly alter the macroscopic foam structure, although Pd–PVP shows brighter spots consistent with metal nanoparticles at or near the polymer surface.

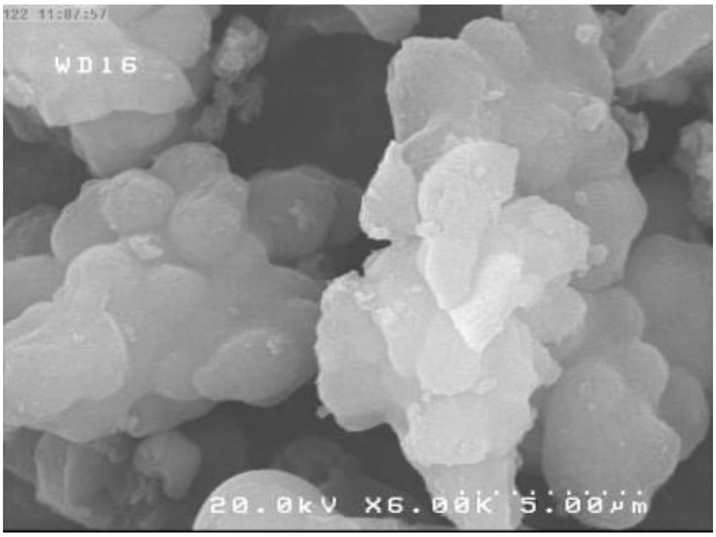

Fig. 8. Scanning Electron Microscopy (SEM) Image of Mesocellular Silica MCF

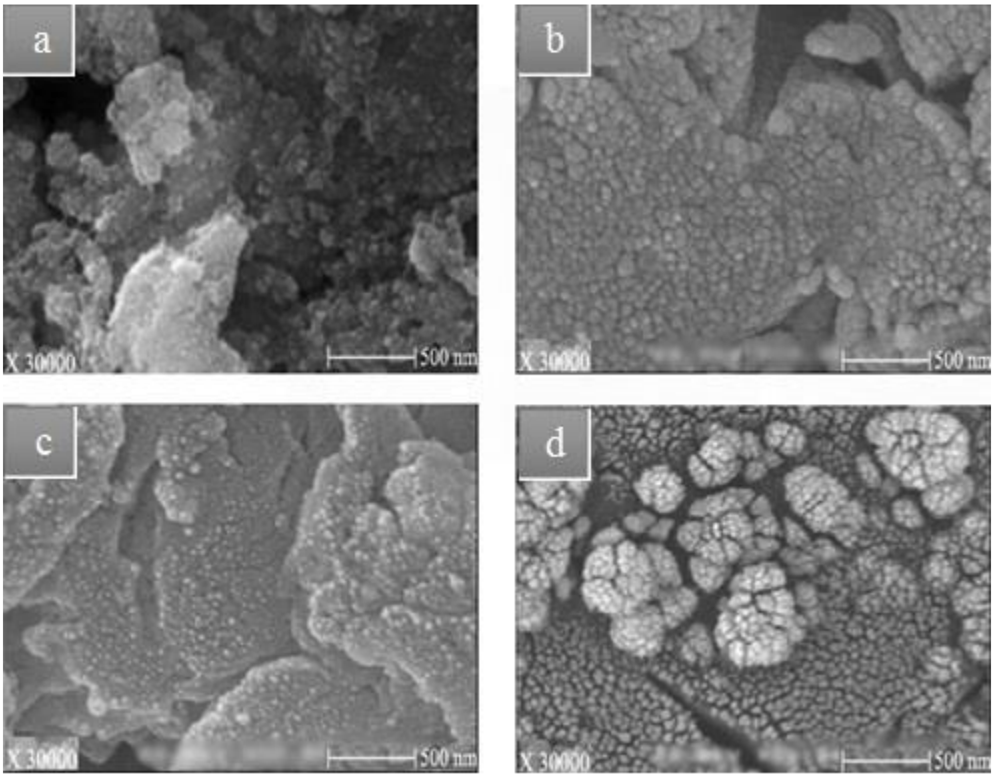

Fig. 9. Scanning Electron Microscopy (SEM) Images at 30,000× Magnification: (a) MCF, (b) PVP/MCF, (c) Mesocellular PVP, (d) Pd-PVP

TEM images of Pd–PVP (Figure 10) reveal dark contrast spots assigned to Pd nanoparticles dispersed within and on the surface of the mesocellular polymer. Smaller, less contrasted particles (3–5 nm) are embedded within the PVP cavities, while larger particles (5–15 nm) reside on the external surfaces of the mesocells. This bimodal distribution suggests that both internal and external polymer sites participate in metal stabilization, which is advantageous for maximizing utilization of Pd active sites.

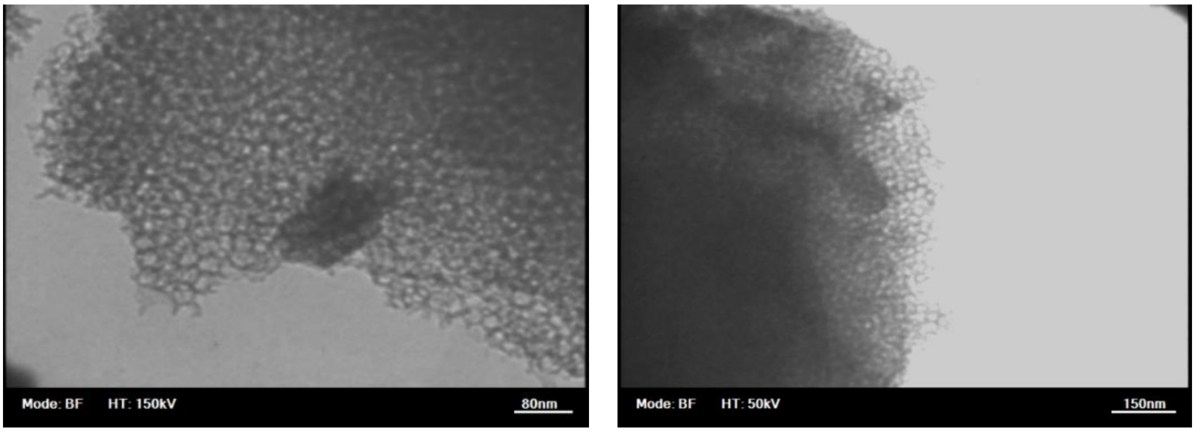

Fig. 10. Transmission Electron Microscopy (TEM) Image of Pd-PVP

3-7- UV–Vis Spectroscopy

Solid-state UV–Vis spectra of $Pd(OAc)_2$ and Pd–PVP are shown in Figures 11 and 12. $Pd(OAc)_2$ displays an absorption band around 400 nm characteristic of Pd^{2+} d–d transitions. In the spectrum of Pd–PVP, this band disappears, and no new features attributable to Pd^{2+} are observed, indicating that Pd^{2+} has been almost completely reduced to Pd^0 [4,5]. Combined with XRD and TEM results, these data confirm successful in situ formation of metallic Pd nanoparticles stabilized by the PVP framework.

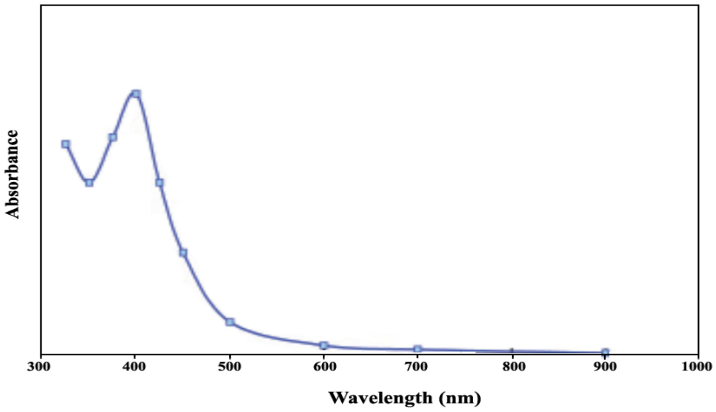

Fig. 11. Solid-State UV-Vis Spectrum of $Pd(OAc)_2$

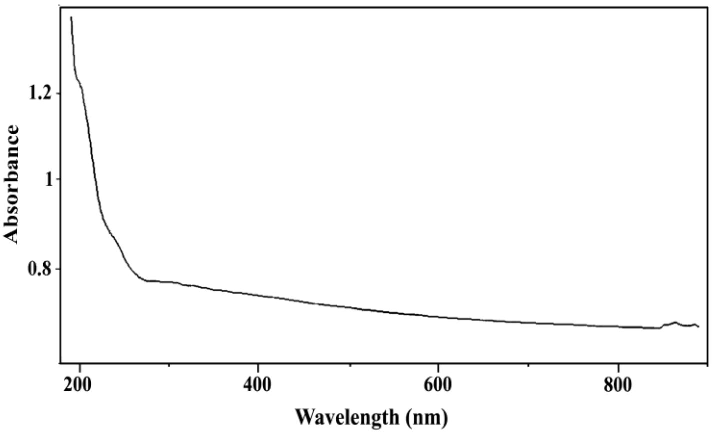

Fig. 12. Solid-State UV-Vis Spectrum of the Pd-PVP Nanohybrid

3-8- Catalytic Oxidation of Toluene: Effect of Solvent and Temperature

The Pd–PVP nanohybrid was evaluated as a heterogeneous catalyst for the oxidation of toluene to benzyl alcohol using H_2O_2 or TBHP as oxidant. Solvent and temperature strongly influence both conversion and selectivity. Systematic screening was performed using water, ethanol, acetonitrile, dioxane, and a water/ethanol (1:3 v/v) mixture in the temperature range from room temperature to 80 °C. As summarized in Table 2, water provides the highest yields and selectivity to benzyl alcohol at room temperature and 50 °C, with conversions up to 95–97% within 2–3 h. Mixed aqueous–organic systems and neat organic solvents give lower yields and/or longer reaction times, likely due to decreased solubility of H_2O_2 and altered interactions between the hydrophobic substrate and the polymeric surface. The superior performance in water is notable, as many traditional oxidation catalysts require organic solvents [1–3,6].

Table 2. Effect of Solvent and Temperature on the Oxidation of Toluene Catalyzed by Pd-PVP

Solvent	Temperature	Reaction Time (h)	Yield (%)
Water	Room temp	3	95
Water	50°C	2	97
Water–Ethanol (1:3)	Room temp	3	92
Water–Ethanol (1:3)	50°C	2	95
Ethanol	Room temp	4	85
Acetonitrile	Room temp	4	82
Dioxane	Room temp	5	60

Interestingly, raising the temperature from room temperature to 50 °C accelerates the reaction but may slightly promote over-oxidation to benzaldehyde and benzoic acid in some cases. Under optimized conditions (water, room temperature), selectivity towards benzyl alcohol remains high, consistent with a mild oxidation pathway mediated by surface-bound Pd and active oxygen species derived from H_2O_2 [7,8].

3-9- Effect of Base

The presence of a base significantly affects the reaction rate and product distribution. Using K_2CO_3, Na_3PO_4, and triethylamine under otherwise identical conditions, K_2CO_3 affords the highest yield of benzyl alcohol (up to 97%), while Na_3PO_4 and Et_3N result in lower conversions (Table 3). The superior performance of inorganic carbonate is consistent with literature reports on Pd-catalyzed oxidation of benzylic substrates, where moderately basic conditions facilitate deprotonation and activation of the benzylic C–H bond without excessively promoting over-oxidation or decomposition of H_2O_2 [6,8].

Table 3. Effect of Base on the Oxidation of Toluene in the Presence of Pd-PVP

Entry	Base	Yield (%)
1	K_2CO_3	97
2	Na_3PO_4	75
3	Et_3N	40

3-10- Effect of Catalyst Loading

Varying the amount of Pd–PVP from 0.06 to 0.14 g (based on 1 mmol toluene and fixed oxidant loading) reveals a strong dependence of reaction rate on catalyst loading (Table 4). At 0.06 g, the reaction is relatively slow (7 h, 70% yield), while increasing the catalyst amount to 0.10 g reduces the reaction time to 5 h with a 95% yield. An optimum is observed at 0.12 g, where 97% yield is achieved within 3.5 h. Further increase to 0.14 g does not provide significant additional benefit, indicating that above a certain dispersion threshold, the reaction becomes limited by mass transport and/or oxidant availability rather than the number of active sites.

Table 4. Effect of Catalyst Amount on the Oxidation of Toluene Using Pd-PVP

Entry	Catalyst Amount (g)	Reaction Time (h)	Yield (%)
1	0.06	7	70
2	0.10	5	95
3	0.12	3.5	97
4	0.14	3.5	97

These findings align with previous observations on heterogeneous Pd catalysts in benzylic oxidations, where an optimal combination of particle size, dispersion, and metal loading yields maximum turnover frequencies [7,18,23].

3-11- Substrate Scope: Oxidation of Toluene Derivatives

To explore the applicability of Pd–PVP, several substituted toluenes were subjected to oxidation under the optimized conditions (water, room temperature, K_2CO_3 base, 0.12 g catalyst, H_2O_2 oxidant). As summarized in Table 5, toluene, 4-methyl toluene, and 2-chlorotoluene are converted to the corresponding benzyl alcohols with high yields (90–97%) within 3.5–5 h. The slightly lower yield for 2-chlorotoluene can be attributed to steric and electronic effects that influence the rate of benzylic C–H activation.

The good performance across different substituents indicates that the Pd–PVP catalyst can accommodate varying electronic environments and steric demands, and that the mesocellular pores provide sufficient space for diffusion and binding of substituted aromatic substrates.

Table 5. Oxidation of Various Toluene Derivatives Catalyzed by Pd-PVP Under Optimized Conditions

Entry	Substrate	Product	Time (h)	Yield (%)
1	Toluene	Benzyl alcohol	3.5	97
2	4-Methyl toluene	4-Methylbenzyl alcohol	4	95
3	2-Chlorotoluene	2-Chlorobenzyl alcohol	5	90

3-12- Catalyst Recyclability and Stability

Reusability is a key requirement for practical heterogeneous catalysts. The Pd–PVP nanohybrid was tested for eight consecutive cycles of toluene oxidation under identical conditions. After each run, the catalyst was separated, washed with water and organic solvents, dried, and reused. The catalytic activity and selectivity remained essentially unchanged over eight cycles, with only a marginal decrease in conversion.

ICP-AES analysis indicates that the Pd content decreases slightly from 0.123 to 0.103 mmol g^{-1} after eight cycles, corresponding to minimal metal leaching(**Table 6)**. The preserved performance compares favorably with other Pd-based oxidation catalysts operating in aqueous media and underscores the stabilizing effect of the PVP matrix and mesocellular architecture [10–11,8,24].

Table 6. Recyclability of Pd-PVP Catalyst in the Oxidation of Toluene

Entry	Cycle Number	Yield (%)	Pd Content (mmol g^{-1})*
1	Fresh	97	0.123
2	1	97	0.123
3	2	96	0.120
4	3	96	0.118
5	4	95	0.115
6	5	95	0.112
7	6	94	0.110
8	7	94	0.106
9	8	93	0.103

This table 7 summarizes the main oxidation strategies reported for the conversion of toluene to benzaldehyde. Based on these results, our result were bether than reported results.

Table 7. Comparison of different reported methods for the selective oxidation of toluene to benzaldehyde.

No.	Oxidation Method	Oxidant / Catalyst	Typical Reaction Conditions	Yield / Selectivity	Ref.
1	TBHP-based oxidation	TBHP / Cu, Fe, Co catalysts	60–100 °C	High yield and selectivity	31
2	Photocatalytic oxidation	TiO_2, g-C_3N_4 + O_2	UV or visible light	High selectivity, low conversion	32
3	Electrochemical oxidation	Carbon or metal electrodes	Ambient temperature	Tunable selectivity	33
4	Nanocatalytic oxidation	Au, Pd, Cu nanoparticles	Mild conditions, O_2 or H_2O_2	Very high selectivity	34
5	Nanocatalytic oxidation	Pd Nanohybride	H_2O_2	High yield and selectivity	This work

4- Conclusion

A mesocellular PVP-based Pd nanohybrid catalyst (Pd–PVP) was successfully synthesized via a nanocasting approach using MCF as a hard template, followed by in situ coordination and reduction of Pd^{2+} ions. Comprehensive characterization confirmed the formation of a well-defined mesocellular polymer with uniformly dispersed Pd^0 nanoparticles stabilized by PVP functional groups.

In the selective oxidation of toluene to benzyl alcohol using H_2O_2 in water, Pd–PVP exhibited high activity and selectivity under mild conditions. Water was identified as the optimal solvent, K_2CO_3 as the most effective base, and an intermediate catalyst loading (0.12 g per mmol toluene) provided the best compromise between conversion and catalyst utilization. The catalyst tolerated different toluene derivatives and could be reused for at least eight cycles with negligible loss of performance and minimal Pd leaching.

The combination of a fully organic mesocellular framework and strongly coordinated Pd nanoparticles offers a promising strategy for designing robust, recyclable oxidation catalysts operating in green media. The approach presented here can be extended to other POP architectures and metal centers for a wide range of selective oxidation and hydrogenation processes.

References

[1] R. A. Sheldon, “E factors, green chemistry and catalysis: an odyssey,” Chem. Commun., vol. 2008, 2008.

[2] G. J. ten Brink, I. W. C. E. Arends, and R. A. Sheldon, “Green catalytic oxidation of alcohols in water,” Science, vol. 287, 2000.

[3] S. A. C. Carabineiro, “Supported gold nanoparticles as catalysts for the oxidation of alcohols and alkanes,” Catalysts, vol. 9, 2019.

[4] W. Hou, N. A. Dehm, and R. W. J. Scott, “Alcohol oxidations in aqueous solutions using Au, Pd, and bimetallic Au–Pd nanoparticle catalysts,” J. Catal., vol. 253, 2008.

[5] J. W. Farag et al., “Catalytic activity of water-soluble palladium nanoparticles for environmentally friendly oxidation of organic substrates,” Nanomaterials, vol. 15, 2025.

[6] H. Targhan et al., “Palladium-based pseudohomogeneous catalyst for highly efficient aerobic oxidation of alcohols,” Sci. Rep., vol. 14, 2024.

[7] J. Xu et al., “Palladium nanoparticles supported on mesoporous carbon nitride for efficient selective oxidation of benzyl alcohol with molecular oxygen,” Appl. Catal. A, vol. 542, 2017.

[8] B. Donoeva, N. Masoud, and P. E. de Jongh, “Colloidal Au catalyst preparation: selective removal of stabilizer (PVP) by oxalic acid,” ACS Catal., vol. 8, 2018.

[9] G. H. Han et al., “Effect of polyvinylpyrrolidone on palladium catalysts for direct H_2O_2 synthesis from H_2 and O_2,” RSC Adv., vol. 10, 2020.

[10] G. Collins et al., “Stability, oxidation and shape evolution of PVP-capped Pd nanocrystals,” J. Phys. Chem. C, vol. 118, 2014.

[11] Z. Wang et al., “Solvent-free selective catalytic oxidation of benzyl alcohol over Pd-based catalysts: role of surface Pd^{2+} and nitrogen functionalities,” Catalysts, vol. 15, 2025.

[12] W. Sun et al., “Selective oxidation of toluene to benzyl alcohol catalyzed by F^--modified CuNiAl hydrotalcite compounds,” J. Mol. Catal. A, vol. 27, 2013.

[13] Y. Feng et al., “Selective liquid-phase oxidation of toluene with molecular oxygen over metal oxide catalysts,” Catalysts, vol. 10, 2020.

[14] G. Chen et al., “Solvent-free liquid-phase selective catalytic oxidation of toluene to benzyl alcohol and benzaldehyde over CeO_2–MnO_x composite oxides,” React. Chem. Eng., vol. 7, 2022.

[15] Z. Li et al., “Rational design of S-scheme CdS/MnO_2 heterojunctions for efficient and selective

oxidation of toluene to benzyl alcohol and benzaldehyde," Chem. Eng. J., vol. 470, 2025.

[16] S. Gao et al., "Selective heterogeneous photocatalytic activation for the oxidation of toluene into value-added products," Catal. Sci. Technol., vol. 15, 2025.

[17] S. C. Kim et al., "Complete oxidation of toluene over supported palladium catalysts: effect of support," Korean J. Chem. Eng., vol. 33, 2016.

[18] W. Tan et al., "$Ce_{0.6}Zr_{0.3}Y_{0.1}O_2$ nanorod-supported Au–Pd nanoparticles: high-performance catalysts for toluene oxidation," Nanoscale, vol. 7, 2015.

[19] P. Schmidt-Winkel, W. W. Lukens, and D. Zhao, "Mesocellular siliceous foams with uniformly sized cells and windows," J. Am. Chem. Soc., vol. 121, 1999.

[20] D. Zhao, Q. Huo, and J. Feng, "Triblock copolymer syntheses of mesoporous silica with periodic 50 to 300 Å pores," Science, vol. 279, 1998.

[21] L. Hermida et al., "Large-pore mesostructured cellular foam (MCF) silica: synthesis, properties and applications—a review," Open Chem., vol. 17, 2019.

[22] A. Chrzanowska et al., "Mesocellular silica foams (MCFs) with tunable pore size as carriers for lysozyme adsorption," Int. J. Mol. Sci., vol. 21, 2020.

[23] K. Grzelak et al., "Ce- and Ca/Nb-doped Pd–mesocellular foam catalysts: structure and performance in oxidation reactions," Appl. Catal. A, vol. 617, 2021.

[24] C. Xu et al., "Porous organic polymers: an emerged platform for photocatalytic water splitting," Front. Chem., vol. 6, 2018.

[25] L. Yang et al., "Design and synthesis of porous organic polymers for catalytic applications," Polymers, vol. 15, 2023.

[26] H. Wang et al., "Porous organic polymers supported heterogeneous catalysts: recent advances and perspectives," Eur. J. Inorg. Chem., vol. 2024, 2024.

[27] X. Liu et al., "Porous organic polymers containing active metal centers as catalysts for heterogeneous transformations," Catal. Today, vol. 312, 2018.

[28] D. Skendrović et al., "Mesocellular silica foam as immobilization carrier for 2-deoxyribose-5-phosphate aldolase," Int. J. Mol. Sci., vol. 25, 2024.

[29] M. R. Hill et al., "Internal and external surface characterisation of templating routes to nanocast mesoporous silicas and carbons," J. Mater. Chem., vol. 19, 2009.

[30] M. Sridhar, "Template-directed synthesis and characterization of organic mesoporous v

[31] Parmeggiani, C.; Cardona, F. Transition-Metal-Based Catalysts in the Aerobic Oxidation of Alcohols. Green Chemistry, 2012, 14, 547–564.

[32] Gupta, K. C.; Sutar, A. K. Selective Oxidation of Toluene to Benzaldehyde Using Metal Catalysts. Applied Catalysis A: General, 2008, 334, 193–201.

[33] Li, X.; Chen, J. Selective Oxidation of Toluene with Hydrogen Peroxide. Journal of Molecular Catalysis A: Chemical, 2010, 323, 1–7.

[34] Zhang, Y.; Wang, L.; Li, G. Photocatalytic Oxidation of Toluene over TiO_2-Based Catalysts. Applied Catalysis B: Environmental, 2015, 165, 715–722.